Neuroscience 344 (2017) 346–359

ALTERED FRONTO-STRIATAL FUNCTIONS IN THE *GDI1*-NULL MOUSE MODEL OF X-LINKED INTELLECTUAL DISABILITY

LORENZO MORÈ,[a†] BASIL KÜNNECKE,[b] LATEFA YEKHLEF,[c] ANDREAS BRUNS,[b] ANTONELLA MARTE,[d†] ERNESTO FEDELE,[d] VERONICA BIANCHI,[a] STEFANO TAVERNA,[c] SILVIA GATTI[b†] AND PATRIZIA D'ADAMO[a*]

[a] *Molecular Genetics of Intellectual Disability Unit, Division of Neuroscience, IRCCS San Raffaele Scientific Institute, Milan, Italy*

[b] *pRED, Pharma Research & Early Development, NORD Neuroscience, Roche Innovation Center Basel, F. Hoffmann-La Roche AG, Switzerland*

[c] *Neuroimmunology Unit, IRCCS San Raffaele Scientific Institute, Milan, Italy*

[d] *Department of Pharmacy, Section of Pharmacology and Toxicology, Center of Excellence for Biomedical Research, University of Genoa, Genoa, Italy*

Abstract—RAB-GDP dissociation inhibitor 1 (*GDI1*) loss-of-function mutations are responsible for a form of non-specific X-linked Intellectual Disability (XLID) where the only clinical feature is cognitive impairment. *GDI1* patients are impaired in specific aspects of executive functions and conditioned response, which are controlled by fronto-striatal circuitries. Previous molecular and behavioral characterization of the *Gdi1*-null mouse revealed alterations in the total number/distribution of hippocampal and cortical synaptic vesicles as well as hippocampal short-term synaptic plasticity, and memory deficits. In this study, we employed cognitive protocols with high translational validity to human condition that target the functionality of cortico-striatal circuitry such as attention and stimulus selection ability with progressive degree of complexity. We previously showed that *Gdi1*-null mice are impaired in some hippocampus-dependent forms of associative learning assessed by aversive procedures. Here, using appetitive-conditioning procedures we further investigated associative learning deficits sustained by the fronto-striatal system. We report that *Gdi1*-null mice are impaired in attention and associative learning processes, which are a key part of the cognitive impairment observed in XLID patients.

Key words: X-linked Intellectual Disability, *Gdi1*-null mice, appetitive conditioning, excitatory synapses, fronto-striatal synaptic plasticity.

INTRODUCTION

Intellectual Disability (ID) accounts for 1–2% of the human population (Lubs et al., 2012; Srivastava and Schwartz, 2014). In some cases, the ID phenotype could be part of a syndrome (the syndromic forms such as the Down syndrome) or to be the only clinical manifestation, defined as non-syndromic ID. Genetic studies on large ID families' revealed many genes on the X-chromosome (XLID), explaining the huge incidence on male patients (Ropers and Hamel, 2005). ID is defined by significant limitation in both intellectual functioning and adaptive behavior. Intellectual functioning is referred to mental abilities such as reasoning, problem-solving, abstract thinking, judgment and learning from experience instead adaptive behavior concerned conceptual, social and practical skills (Schalock et al., 2011). Specific aspects of executive functions and conditioned response, which are controlled by fronto-striatal circuitries, are consistently reported to be altered in ID patients (Baker et al., 2011; Bexkens et al., 2014a, 2014b). Recent work on cognitive impairment in animal models of XLID genes have reported memory deficits in trace fear conditioning, inhibition avoidance, extinction and reversal learning. However, defining other aspects like attention and stimulus selection in XLID mouse models might be relevant to the pathology and could provide powerful translational measurements.

One of the first identified X-linked gene to cause human XLID was the guanine nucleotide dissociation inhibitor, *GDI1* (D'Adamo et al., 1998). It encodes for the brain-enriched protein RAB-GDP dissociation inhibitor alpha (αGDI), a protein that controls the cycling of RAB GTPases, a class of small GTPases directly involved in intracellular vesicular trafficking (Grosshans et al., 2006). Previous work on *Gdi1*-null mice reported normal explorative and motivational behavior as well as motor coordination but revealed impaired hippocampal-dependent forms of memory (D'Adamo et al., 2002). Moreover, the major cause of *Gdi1*-null mice cognitive deficit has to be ascribed to alterations in the total number

*Corresponding author. Address. San Raffaele Scientific Institute, Via Olgettina, 58, 20132 Milan, Italy. Fax: +39-02-26434844.
E-mail address: dadamo.patrizia@hsr.it (P. D'Adamo).
† Current addresses: School of Life Sciences, University of Warwick, CV4 7AL Coventry U.K. (L. Morè). Department of Experimental Medicine, University of Genoa, Genoa, Italy (A. Marte). Institut de Recherche Pierre Fabre, Toulose, France (S. Gatti).

Abbreviations: αGDI, RAB GDP dissociation inhibitor alpha; CI, conditioned inhibition; CS, conditioned stimulus; EPSCs, excitatory postsynaptic currents; fMRI, functional magnetic resonance imaging; LI, latent inhibition; mPFC, medial prefrontal cortex; MSNs, medium spiny neurons; Pr, release probability; RRP, ready releasable pool; SV, synaptic vesicles; US, unconditioned stimulus; VTA, ventral tegmental area; XLID, X-linked Intellectual Disability.

http://dx.doi.org/10.1016/j.neuroscience.2016.12.043
0306-4522/

of hippocampal and cortical synaptic vesicles (SV) during postnatal synaptic differentiation. In adult mice the distribution of SV is altered in differentiated neuronal terminals, and the reserve pool appears to be specifically affected. This results in a slow recovery after SV depletion, which leads to a memory deficit whenever the synaptic SV demand should increase both with task duration and task difficulty (Bianchi et al., 2009). Neuropsychological and imaging analysis in *GDI1*-mutated patients, with non-specific XLID, revealed a mean intelligent quotient (IQ) of 45 (moderate ID) and functional brain alteration suggesting impairment of cerebello-thalamo-frontal pathway (Curie et al., 2009).

Thus, we asked whether *Gdi1*-null mice might reveal deficits due to a reduced inhibitory action of the frontal cortex (FC) on the basal ganglia leading to a lack of selective attention (Pezze et al., 2009; Kahn et al., 2012). In the present study, inhibitory processes and attention were systematically evaluated in the *Gdi1*-null mouse using a battery of newly developed set of behavioral procedures able to define the prominence of fronto-striatal functional deficits, similar to those reported in ID patients (Curie et al., 2016). Moreover, we used functional magnetic resonance imaging as a translational approach to obtain an integral view of neuro-functional alterations in the *Gdi1*-null brain and potentially link these to the cognitive deficits. Finally, behavioral and functional readouts were supported by electrophysiological and neurochemical investigations that addressed the cellular alterations and provided specific evidence of a major involvement of the glutamatergic system also in the fronto-striatal pathway.

EXPERIMENTAL PROCEDURES

Animals

Male *Gdi1*$^{-/Y}$ mice and *Gdi1*$^{+/Y}$ littermates (denoted *Gdi1*-null and *Gdi1* WT for simplicity) (D'Adamo et al., 2002) were used for this study. All efforts were made to minimize animal suffering and to reduce the number of mice used, in accordance with the European Communities Council Directive of November 24, 1986 (86/609/EEC) and the subsequent Italian Law on the "Protection of animal used for experimental and other scientific reasons". All procedures on animals reported here were approved by both the Department of Biotechnologies (DIBIT) Institutional Animal Care (Milan, Italy) and by the National Ministry of Health (IACUC #653).

Animal used in behavioral procedures

Behavioral analysis started at the age of 3 months and mice were housed in pairs and had water freely available in the home-cage. The holding room was on a 12-h light–dark cycle (lights on from 8.00 pm to 8.00 am). All experiments were carried out during the dark phase of the cycle. Food-deprived mice (maintained at 85% of their free-feeding weight) were weighed twice a day, before and at the end of the experimental session. Food restriction started one week before the beginning of the experiment and mice were fed with a restricted daily ration of food at the end of each experimental session. Before the start of an experiment mice were exposed to the food pellets (in

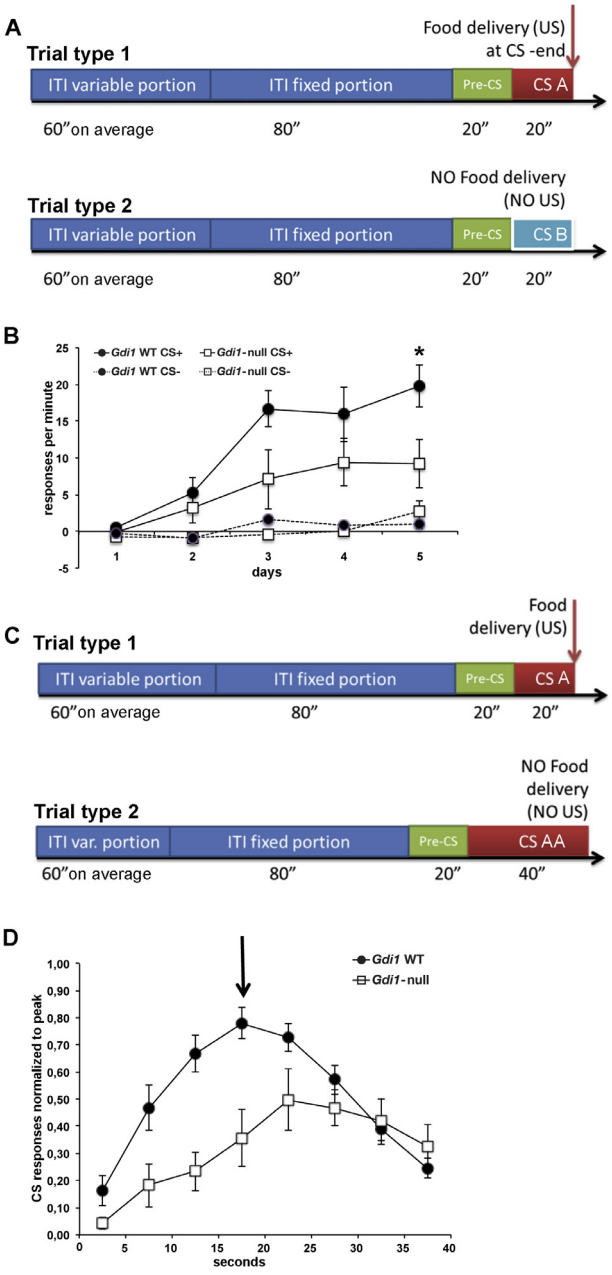

Fig. 1. Discriminative Delay Conditioning and Peak procedure. (A) Schematic representation of the protocol used. In trial type 1, a CS A is paired with food (CS A+; red box) whereas in trial type 2, a CS B is not paired with food presentation (CS B-; light blue box). This experiment lasted 5 days. (B) Responses per minute obtained by subtracting the scores for CS A+ or CS B− from pre-CS (solid lines and dotted lines, respectively). (C) Schematic representation of the protocol used in peak procedure. In trial type 1, a CS A is paired with food whereas in trial type 2, the CS AA is not paired with food presentation. (D) Responses relative to CS AA− (40 s) trial obtained by the peak procedure on all trials pooled together and averaged in blocks of 5 s each. Black arrow indicates the correct mean peak value around 20 s. Values represent the mean ± SEM. $^{*}p < 0.05$. (For interpretation of the references to colour in this figure legend, the reader is referred to the web version of this article.)

their home-cage) and were habituated to the test boxes (1 h/day for 3 days). Five independent cohorts of naïve *Gdi1*-null and WT littermates, each composed of 8 mice per genotype were subjected each to the five behavioral procedures described below. Mice were randomly assigned to the conditioning boxes in order to have 2 *Gdi1*-WT and 2 *Gdi1*-null in each squad and all experiments were conducted with experimenters blinded to genotype.

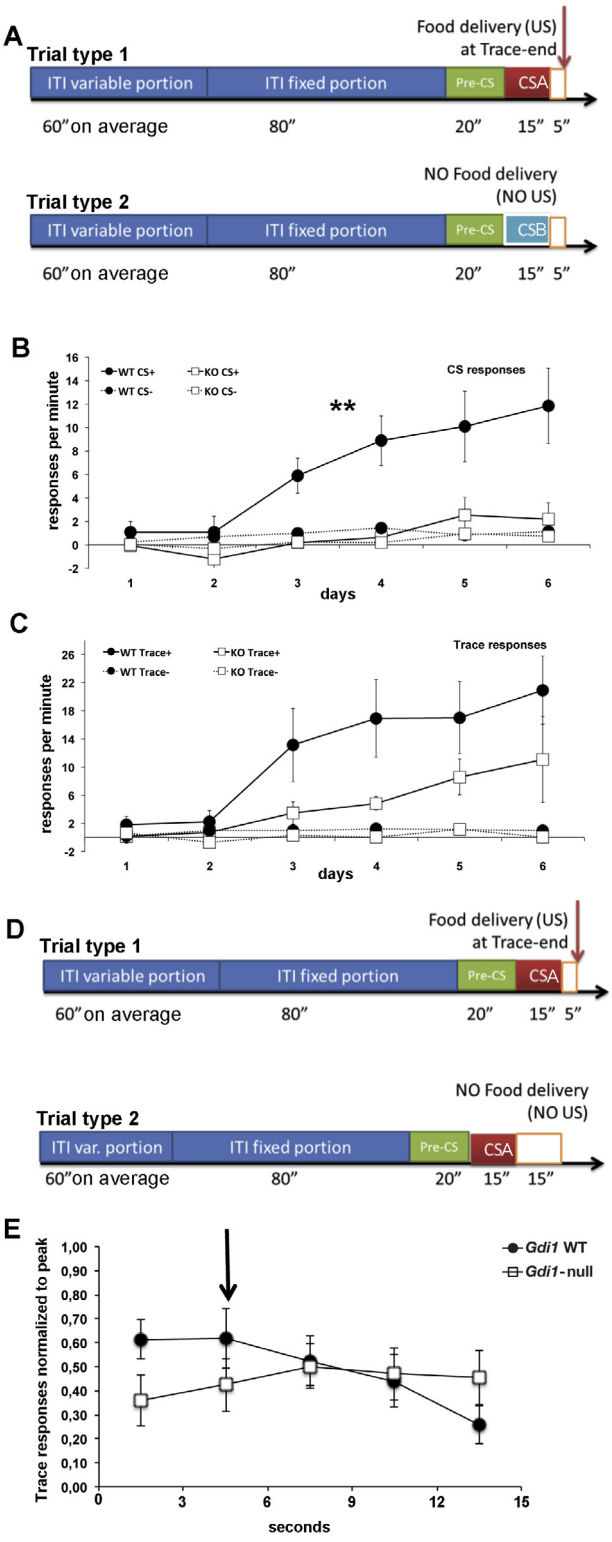

Behavioral apparatus

Experiments were conducted using 4 identical fully automated Classic Modular Test conditioning Chambers for Mouse (Med-Associates Product # ENV-307A). Each of those boxes was housed within an Expanded PVC Sound Attenuating Cubicle (Med-Associates Product # ENV-022V) equipped with a ventilation fan. Mounted in the center of the right wall was a food-tray with an opening measuring 2.5 cm × 2.5 cm × 1.9 cm. This was located 1 cm above the grid floor and was connected to a pellet dispenser through which 14-mg sucrose pellets (Formula P) could be delivered (US). Head entries to the food-tray were detected and recorded by the breaking of an infrared light-beam across the opening. On the top of the food-tray a LED light was placed. At the opposite side of the LED-light there was the house light, a 12-W bulb, mounted in a partially open hood that directed the light upward. The loudspeakers for the presentation of the auditory stimuli were placed in the left wall of the chamber. Employed stimuli were the house-light, the LED-light (CS C) and two pure sounds at 4-kHz and 9-kHz (CS A and B counterbalanced between squads). Med-PC for Windows controlled all the experimental events, and recorded the time at which events occurred with 10-ms resolution.

Fixed time intervals and stimuli present in all behavioral procedure

All behavioral procedures described below (represented schematically in Figs. 1A, C; 2A, D; 3A, C; 4A, B, D, E), are composed by so defined trial type that always started with a variable Inter Trial Interval (ITI; 60 s on average), necessary to perturb mice's responses based on the average cycle time of reinforce deliveries (US: food) (Balsam et al., 2006), and followed by a fixed ITI of 100 s (ITI 80 s + pre-CS 20 s). The called "pre-CS" (the last 20 s of the ITI before the CS) served as measure of uncorrected anticipatory response immediately preced-

Fig. 2. Discriminative Trace Conditioning and Trace Peak procedure. (A) Schematic representation of the protocol used. In trial type 1, a CS A is paired with food (CS+; red box) whereas in trial type 2, a CS B is not paired with food presentation (CS−; light blue box). Empty orange boxes following the CSs are the 5 s trace period. This experiment lasted 6 days. (B) Responses per minute for CSs obtained by subtracting the scores for CS A+ or CS B− from pre-CS (solid lines and dotted lines, respectively). C) Responses per minute for trace+ or trace− obtained by subtracting the score for the trace period from pre-CS. (D) Schematic representation of the protocol used in peak procedure. In trial type 1, a CS A is paired with food after the trace (empty orange box) whereas in trial type 2, the CS A is not paired with food presentation after a longer trace period (15 s). E) Responses relative to trace period (15 s) obtained by the peak procedure on all trials pooled together and averaged in blocks of 3 s each. Black arrow indicates the correct mean peak value around 5 s. Values represent the mean ± SEM. $^{**}p < 0.01$. (For interpretation of the references to colour in this figure legend, the reader is referred to the web version of this article.)

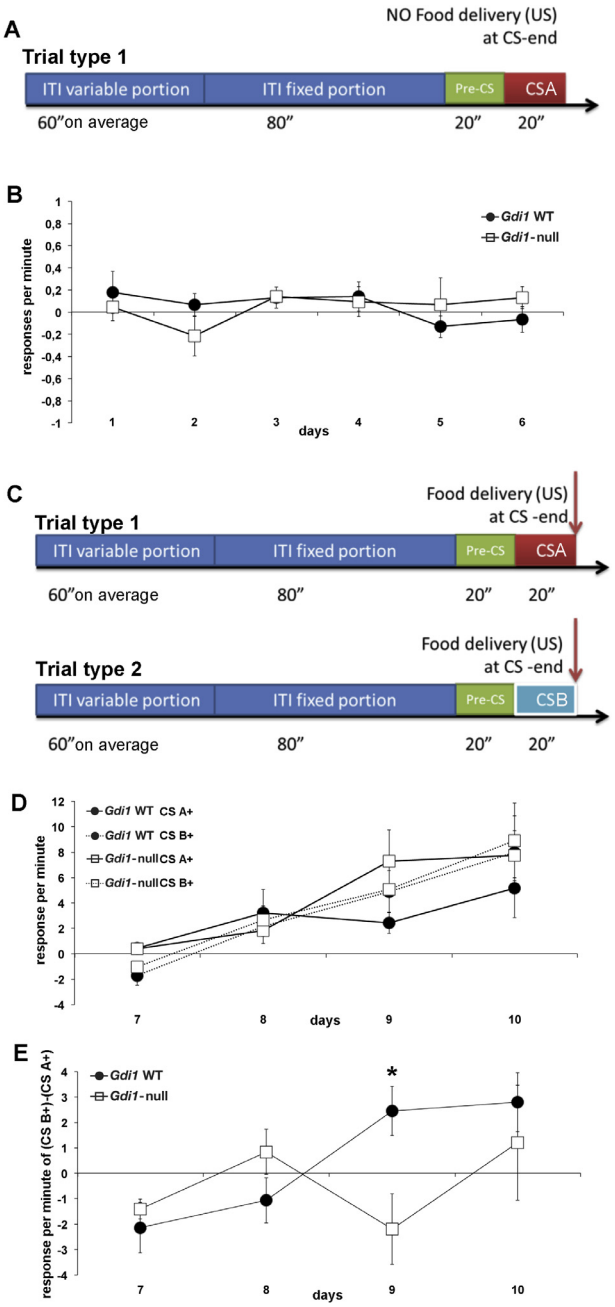

Fig. 3. Latent Inhibition. (A) Schematic representation of the pre-exposure phase. A CS A is not paired with food presentation (CS−; red box). (B) Responses per minute for CS obtained by subtracting the scores for CS A− from pre-CS. (C) Schematic representation of the acquisition phase where the pre-exposed stimulus (CS A; red box) and a second novel stimulus (CS B; light blue box) were paired with food delivery. (D) Responses per minute for CSs obtained by subtracting the scores for CS A+ or CS B+ from pre-CS (solid lines and dotted lines, respectively). (E) Difference scores relative to the NON pre-exposed CS B minus the pre-exposed CS A. Values represent the mean ± SEM. $^{*}p < 0.05$. (For interpretation of the references to colour in this figure legend, the reader is referred to the web version of this article.)

ing each CS presentation. Number and presentation of trial types are specified in each procedure.

The duration and type of CSs is specified in each procedure. CSs could be paired with food reward (+) or not (−).

Dependent variable analyzed in all behavioral procedures

Head entries into the food-tray were measured during CSs and trace intervals. We also scored head entry into the food-tray during the "pre-CS", immediately preceding each CS presentation, as a baseline measure. The measure of conditioning for each type of procedure was then calculated as (if not otherwise stated) responses per minute during the CS period minus responses during the pre-CS period and pooled over all trials in a given session.

Discriminative delay conditioning procedure

To evaluate associative memory, two different trials types, type 1 (CS A+) and type 2 (CS B−), were designed (Fig. 1A). The MED-PC software delivered 30 trials for each trial type in a random way for every daily session. The procedure was repeated for five consecutive days. The CS presentation was of 20 s in duration.

Discriminative delay conditioning and peak procedure

To evaluate timing behavior, after a different discriminative delay conditioning experiment lasting only four days, mice were subjected for four more consecutive days to two randomly assorted trial types: trial type 1 (40 trials) and trial type 2 (20 trials) – the peak procedure task (Fig. 1C).

Trial type 1 was exactly as described above, and used in order to maintain mice responding; while trial type 2 was as trial type 1 but differing on CS duration in the way that it did not stop after 20 s but kept going for a total of 40 s and no food was presented. This is called a peak procedure trial. Data from the peak procedure trials were collected and then each 1-s bin was divided by the highest value of response (the peak value), in order to normalized the average response, and then averaged over 5 s. This way, the highest response in distribution was equal to 1, and each mouse contributed equally to the shape of the distribution regardless of its overall response rate.

Discriminative trace conditioning and peak procedure

To evaluate how a time gap between CS and US could affect associative learning, an interval of 5 s (a trace) between the CSs and US was introduced, on a procedure design called discriminative trace conditioning (Fig. 2A). During the discriminative trace conditioning experiment, MED-PC software delivered 30 trials for each trial type in a random way in every daily session, this stage of the experiment was repeated for six consecutive days. The CS presentation was of 15 s followed by 5 s trace and CS A+ in trial type 1 or CS B− in trial type 2. After this acquisition stage, mice were subjected to the peak procedure for the trace, which lasted for four days. Two randomly assorted trial types: trial type 1 (40 trials) and trial type 2 (20 trials) – the

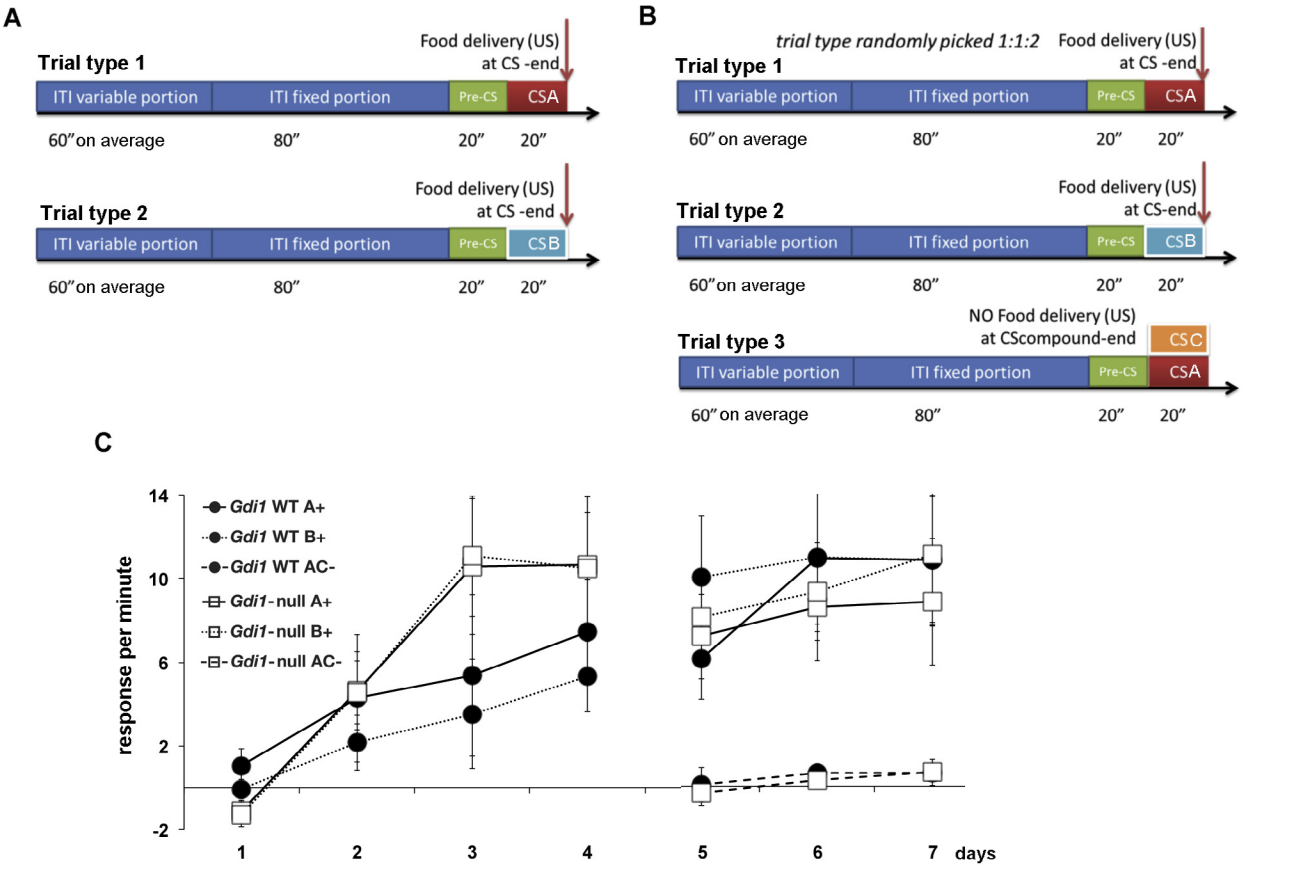
A
Trial type 1
Food delivery (US) at CS -end
ITI variable portion
ITI fixed portion
Pre-CS
CSA
60″on average
80″
20″
20″
Trial type 2
Food delivery (US) at CS -end
CSB
B
trial type randomly picked 1:1:2
Trial type 1
Food delivery (US) at CS -end
Trial type 2
Food delivery (US) at CS-end
Trial type 3
NO Food delivery (US) at CScompound-end
CSC
C
response per minute
Gdi1 WT A+
Gdi1 WT B+
Gdi1 WT AC-
Gdi1-null A+
Gdi1-null B+
Gdi1-null AC-
days
D
Trial type 4
NO Food delivery (US) at CS-end
Trial type 5
NO Food delivery (US) at CScompound-end
E
Trial type 6
Food delivery (US) at CS-end
F
Gdi1 WT
Gdi1-null
suppression ratio = BC/(B + BC)
day 8
G
Gdi1 WT C+
Gdi1-null C+
**
response per minute
days

peak procedure task (Fig. 2D). Trial type 1 was exactly as described above, and used in order to maintain mice responding; while trial type 2 was as trial type 1 but differing on trace duration which here was 15-s long and was not rewarded (instead of being 5-s long and followed by a food pellet). Measures of conditioning were calculated as in discriminative delay conditioning and peak procedures described above, except for the averages of the responses in the peak-procedure, which were computed over bins of three seconds each.

Latent inhibition procedure

To evaluate loss of attention to irrelevant stimuli, mice were first exposed to a non-food rewarded CS and assessed for their background responding (Fig. 3A). Forty trials (trial type 1) a day were presented for six consecutive days, these consisted of a 20-s CS A not food rewarded.

In the second stage of the procedure, the same mice were subjected to two different trial types: trial type 1 now paired with food CS A+ and trial type 2, a new stimulus also paired with food CS B+. MED-PC software delivered 20 trials for each trial type in a random way a day, and the entire stage lasted 4 days (Fig. 3C). This protocol aimed to test the inhibitory effect of a previous learnt outcome of a CS (A−) when in a second stage of the experiment, it was associated with food, leading to a slower learning for this CS (A) compared to a new CS B +(which was never pre-exposed).

The CS presentation was of 20 s in duration.

Conditioned inhibition

To deeply evaluate attention and more active inhibitory processes, mice were first subjected to two different trial types: trial type 1, CS A+ and trial type 2, CS B+, 20 trials each, randomly delivered, for four consecutive days, exactly as the second stage of latent inhibition protocol (Fig. 4A).

On the next three consecutive days, three trial types were now randomly presented with the introduction of a new trial type, as a compound CS: CS AC− (where C was the LED-light) for 30 trials and not food rewarded (Fig. 4B). In that way, the function of the CS AC− presentation is to acquire inhibitory property for C since when A is presented alone it is rewarded but not when it is presented together with C, normally C becomes a conditioned inhibitor.

Following this procedure, mice were then tested in a one-day summation test, with two different trial types: trial type 4, CS B−, and trial type 5, CS BC−, 20 trials each, randomly assorted (Fig. 4D). In that way, the CS C that was never paired before with CS B has the ability to suppress what previously learnt for the CS B+. This is one of the classic ways to assess the strength of a conditioned inhibitor.

Over the next two days, mice were subjected to a retardation test where the conditioned inhibitor CS C was now paired with food. In that way, it is possible to test mice's ability to show the acquired inhibition in the stages before. The retardation test stage was just one trial, type 6, CS C+, 40 trials. Acquired inhibition is here seen as a slower responding to C.

All CS presentations were of 20 s in duration.

Statistical analysis in behavioral procedure

For behavioral procedures, a two-way analysis of variance (ANOVA) or repeated measure ANOVA was used with genotype and day as independent factors (StatView Software; SAS Institute, Cary, NC, USA). T-test was used to analyze single variables. In all statistical tests, the significance level was set at $p < 0.05$. Error bars indicated mean ± S.E.M.

Dopamine release experiment

P2 crude synaptosomal fraction was obtained as described in Raiteri et al. (1984). Briefly, amygdala was dissected from Gdi1 WT (n = 12) and Gdi1-null (n = 12) mice and homogenized in sucrose (0.32 M, 40:1 volume:tissue weight) buffered at pH 7.4 with phosphate (Raiteri et al., 1984). The homogenate was first centrifuged for 5 min at 1,000*g* (4 °C) to remove nuclei and debris and then at 12,000*g* for 20 min (4 °C) to isolate synaptosomes. The P2 synaptosomal pellet was suspended in physiological HEPES-buffered medium with the following composition (mmol/L): NaCl, 140; KCl, 3; MgSO4, 1.2; NaH2PO4, 1.2; HEPES, 10; glucose, 10; pH 7.4). Synaptosomes were subsequently incubated at 37 °C for 15 min with 0.05 μmol/L [7,8-3H]dopamine ([^{3}H]DA, specific activity 90 Ci/mmol, Amersham, Buckinghamshire, UK) in physiological medium containing 0.1 μM/L 6-nitroquipazine and desipramine (Tocris Cookson, Bristol, UK) to block possible entry of [^{3}H]DA into serotonergic and noradrenergic nerve terminals, respectively. After the incubation, equal aliquots of synaptosomal suspension were stratified on Millipore filters present at the bottom of twenty superfusion chambers thermostated at 37 °C and superfusion was accomplished by means of a peristaltic pump (flow rate of 0.5 ml/min). After 36 min of superfusion to reach a steady spontaneous release of [^{3}H]DA, samples of superfusate were

Fig. 4. Conditioned Inhibition. This experiment had four stages. (A) Schematic representation of the acquisition phase (days 1 to 4) where CS A (red box) and a CS B (light blue box) were paired with food delivery. (B) Schematic representation of the subsequent inhibitor training phase (days 5 to 7) where three stimuli were presented: CS A+, CS B+ and AC− where C was the LED-light (orange box). C) Responses per minute for stimuli obtained by subtracting the scores for CS A+ or CS B+ or AC− from pre-CS. (D) Schematic representation of the summation test (day 8) where two stimuli were presented: CS B− and BC− where C was the LED-light (orange box). (E) Schematic representation of the retardation test (days 9 and 10) where the LED-light C (orange box) is rewarded with food. (F) The BC/(BC)+ (B) suppression ratio was employed to represent the results. (G) Responses per minute for light stimulus obtained by subtracting the scores for C+ from pre-CS. Values represent the mean ± SEM. $^{**}p < 0.01$. (For interpretation of the references to colour in this figure legend, the reader is referred to the web version of this article.)

collected in plastic vials according to the following protocol: $t = 36–39$ min pre-depolarization spontaneous release, $t = 39–45$ min KCl-evoked release (a period of 90 s of depolarization was applied at $t = 39$ min with 15 mmol/L KCl), $t = 45–48$ min post-depolarization spontaneous release. Radioactivity present in the fractions collected and in superfused synaptosomes was quantified by liquid scintillation counting.

The amount of [^{3}H]DA present in each fraction collected was expressed as a percentage of the total radioactivity content of present in synaptosomes at the beginning of the respective collection period (fractional rate $\times$ 100). Depolarization-evoked overflow was calculated by subtracting the transmitter content present in the two 3-min fractions (spontaneous pre- and post-depolarization release) from that present in the 6-min fraction collected during and after the depolarization with KCl.

Functional magnetic resonance imaging (fMRI)

Brain imaging was performed in naïve *Gdi1* WT ($n = 7$) and *Gdi1*-null ($n = 11$) mice (age 22–27w) under shallow etomidate anesthesia as described previously (Petrinovic et al., 2016). In brief, anesthesia was induced with 3% isoflurane (Abbott, Baar, Switzerland) in oxygen and air (1:5 v/v), and maintained with etomidate (B. Braun Melsungen AG. Melsungen, Germany) administered intravenously at a rate of 0.75 mg/kg/min. Body temperature was maintained at 37 °C and breathing rate and concentrations of inhaled and exhaled oxygen and CO_2 were continuously monitored on a PowerLab data acquisition system (ADInstruments, Spechbach, Germany).

The fMRI study was conducted on a 9.4 T Bruker Biospec, 20 cm bore animal scanner (Bruker Biospin, Ettlingen, Germany), equipped with a 7-cm-diameter birdcage coil for signal excitation and a surface coil for signal reception. Perfusion imaging as a proxy readout of neural activity was conducted based on the continuous arterial spin-labelling (CASL) method (Centered RARE, TR/TE = 3.75 s/5.4 ms, RARE-factor = 32, 20 mm $\times$ 20 mm field-of-view, 128 $\times$ 64 matrix, 0.6-mm slice thickness, 2 averages, 3-s labeling pulse, 0.4 s post labeling delay). Three sets of perfusion images were collected over 12 min from eight coronal slices positioned at +1.9, +1.0, +0.1, −0.8, −1.7, −2.6, −3.5 and −4.4 mm relative to the bregma. fMRI data were processed and analyzed as described previously (Bruns et al., 2009). Absolute perfusion values obtained from the CASL-images were normalized for each brain area to the mean perfusion of each slice in order to account for possible systemic changes affecting brain perfusion as a whole, and to eliminate part of the inter-individual variability. Normalized blood perfusion in *Gdi1* WT and *Gdi1*-null mice was compared region-wise using two-tailed *t*-tests with no correction for multiple testing. (Given the exploratory character of the present study, we aimed for an assessment subserving hypothesis building rather than a strictly confirmatory analysis.

Electrophysiology in cortico-striatal brain slices

Male mice (60–70 days of age) were anesthetized with an intraperitoneal injection of a mixture of ketamine/xylazine (100 mg/kg and 10 mg/kg, respectively) and perfused transcardially with ice-cold artificial cerebrospinal fluid (ACSF) containing (in mM): 125 NaCl, 3.5 KCl, 1.25 NaH_2PO_4, 2 $CaCl_2$, 25 $NaHCO_3$, 1 $MgCl_2$, and 11 D-glucose, saturated with 95% O_2 and 5% CO_2 (pH 7.3). After decapitation, brains were removed from the skull and 300 μm-thick horizontal cortico-striatal slices were cut in ACSF at 4 °C using a VT1000S vibratome (Leica Microsystems, Wetzlar, Germany). Individual slices were then submerged in a recording chamber mounted on the stage of an upright BX51WI microscope (Olympus, Japan) equipped with differential interference contrast optics (DIC). Slices were perfused with ACSF continuously flowing at a rate of 2–3 ml/min at 32 °C. Whole-cell patch-clamp recordings were performed in neostriatal medium spiny neurons (MSNs) using pipettes filled with a solution containing the following (in mM): 10 NaCl, 124 KH_2PO_4, 10 HEPES, 0.5 EGTA, 2 $MgCl_2$, 2 Na_2-ATP, 0.02 Na-GTP, (pH 7.2, adjusted with KOH; tip resistance: 4–6 MΩ). Excitatory postsynaptic currents (EPSCs) were evoked in MSNs by electrical stimulation of the neocortex using a bipolar tungsten electrode (FHC, Greenville, PA), placed near the external capsule at the border between cortex and neostriatum and connected to a stimulus isolator (WPI Europe, Berlin, Germany). To isolate AMPA-receptor dependent EPSCs, the ACSF was added with the $GABA_A$-receptor antagonist gabazine (10 μM) and recordings were performed at a holding potential of −80 mV.

Paired-pulse protocols were applied using dual stimuli at 50- through 250-ms inter-stimulus intervals in 50-ms increasing steps. Each stimulus lasted 0.2 ms, while current intensity was previously adjusted in order to obtain steady, reliable EPSCs with no failures during low-frequency stimulation (0.1 Hz). Paired-pulse ratios (PPRs) were calculated by dividing the second EPSC peak amplitude by the first one for any paired-pulse sequence. High-frequency stimulus trains (20 Hz, 4 s) were applied to assess SV readily releasable pools (RRPs) (Bianchi et al., 2009). Cumulative EPSC peak amplitudes were plotted and the late phase (20–25 points) of the dataset was linearly fit. Back-extrapolation of the fit line to the Y-axis intercept provided an estimate of the RRP (Schneggenburger et al., 1999). The probability of release (Pr) of any given vesicle in the RRP was calculated as the ratio between the first-evoked EPSC in the train and the RRP size.

All recordings were performed using a MultiClamp 700B amplifier interfaced with a PC through a Digidata 1440A (Molecular Devices, Sunnyvale, CA, USA). The series resistance was partially compensated (40–50%) using the amplifier control circuit. Data were acquired using pClamp10 software (Molecular Devices) and analyzed with Origin 9.1 (Origin Lab, Northampton, MA, USA). Voltage-clamp traces were sampled at a frequency of 30 kHz and low-pass filtered at 2 kHz.

RESULTS

αGDI is expressed in all brain regions and its lack has been previously proven to affect hippocampal, cortical and amygdala glutamatergic synapses in the process of memory formation linked to SVs content defect (D'Adamo et al., 2002; Bianchi et al., 2009). We thus investigate whether *Gdi1*-null mice show more pronounced deficits in tasks with higher SV demand and implicating not only the limbic system but also the fronto-striatal system as observed in ID patients. We subject the animals through different paradigms necessary to evaluate *Gdi1*-null mice responses to task difficulty and based on fronto-striatal system such as discriminative delay conditioning, discriminative trace conditioning, interval-timing behavior, latent inhibition and conditioned inhibition.

Gdi1-null mouse lacks discriminative conditioning over time and are impaired in interval timing behavior

A discriminative delay-conditioning task was employed to test whether *Gdi1*-null mice were able to take the most appropriate action when presented with a food reinforced conditioned stimulus (CS A+) and a non-reinforced CS (CS B−) (Fig. 1A). Both *Gdi1* WT and *Gdi1*-null mice displayed discriminative response to the CS A+ (Fig. 1B, solid lines) over CS B− (Fig. 1B, dotted lines) but a significant interaction between genotypes and days was observed (ANOVA genotype*day: $F[4,1] = 2.5$; $p = 0.049$) and factorial analysis showed a main effect that became significant for day 5 (ANOVA genotype effect: $F[1,14] = 5.9$; $p = 0.03$; Fig. 1B) which indicates a greater discriminative conditioning achieved by *Gdi1*-WT mice. This result demonstrates in a goal tracking procedure that the level of conditioning to a CS predicting a biological relevant stimulus *vs*. a CS, which did not, was greater in *Gdi1* WT than in the *Gdi1*-null mice. We thus conclude that *Gdi1*-null mice are less efficient in engaging the appropriate action with regard to stimuli carrying different qualitative information.

We then subjected a new cohort of *Gdi1* mice to four days discriminative delay conditioning task followed by interval timing behavior procedure in order to investigate the functioning of a key brain structure involved in attention and stimulus processing *i.e.* the frontal cortex and the striatum (Lustig et al., 2005; Meck et al., 2013; Merchant et al., 2013).

As expected, no significant differences were observed between genotype in the responses to the CS A+ over the CS B− after only four days of training (data not shown) allowing thus to switch to a peak procedure (Fig. 1C) under similar conditions for both groups. As shown in Fig. 1D, the response of *Gdi1* WT mice correctly peaked around 20 s, while *Gdi1*-null mice had their peak response later (shifted to the right). The difference between the peak times of the two groups was statistically significant (*Gdi1* WT 17.6 ± 1.17 s, *Gdi1*-null 26.5 ± 2.49 s; *t*-test, $p = 0.002$).

This experiment demonstrates that *Gdi1*-null mice performed poorer in timing a well-known interval as they showed less precision in their peak response and more variability. This result suggests a deficit in processing temporal information that involves the medium spiny neurons in the striatum and frontal cortices (the Beat Frequency Model) (Matell et al., 2003; Meck, 2006; Meck et al., 2008; Petter et al., 2016).12

Gdi1-null mouse exhibits prominent deficits in a Pavlovian discriminative trace-conditioning task

We then subjected a new cohort of mice to discriminative trace conditioning in order to evaluate their ability to take the most appropriate action when presented with different trace interval tasks, one of which was paired with food (CS A+) at trace-end while the other was not (CS B−) (Fig. 2A). The ability to properly respond to trace intervals is of major interest in the field of associative learning and interval timing since behavioral theories make different predictions and this might have profound implications on the translational validity of the tasks between mice and humans. Briefly, Informational processing theories (Gallistel and Balsam, 2014) see the onset of offset of stimuli (when CS switch on and off) as the major information-providing sources. They thus assume that responses during the trace interval should not decay (as we have confirmed).

Both genotypes displayed discriminative response to the CSs (i.e. for the CS whose trace was followed by a reward Fig. 2B) but *Gdi1*-null mice did not achieve the greater discriminative conditioning observed in *Gdi1* WT mice for CS A+ (ANOVA genotype effect: $F[1,14] = 13.45$; $p = 0.002$) (Fig. 2B, solid lines). The same analysis carried out for the trace interval however did not revealed any significant genotype effect (ANOVA genotype effect for trace+: $F[1,14] = 4$; $p = 0.07$) (Fig. 2C).

These results show that *Gdi1* WT mice associated both trace and CS intervals while *Gdi1*-null mice showed poorer associative strength for the longer (15 s vs. 5) and further away interval (the CS is not contiguous with the food reward as in fact the trace is) since this interval carries less information than the Trace (Gallistel and Balsam, 2014).

After 6 days of acquisition, we switched to a trace-peak procedure (Fig. 2D) under similar conditions between groups. Fig. 2E shows that *Gdi1* WT mice had a correct trace-peak response around 5 s, while *Gdi1*-null mice peaked later (peak moved to the right). The difference of the peak times of the two groups was statistically significant (*Gdi1* WT 5.38 ± 1.72 s, *Gdi1*-null 9.63 ± 1.19 s; *t*-test, $p = 0.03$).

This experiment showed a less efficient conditioning in the *Gdi1*-null mice to the longer CS interval while no statistically relevant difference was seen for the shorter trace interval. It also showed that both groups increased their response rate during the trace interval in a similar fashion, which supports information processing models' predictions for which subjects started timing when the CS switched off.

Gdi1-null mouse does not show latent inhibition (LI)

To further evaluate fronto-striatal function we then investigated with LI which is a reliable paradigm that

reflects attentional processes (Lazar et al., 2012; Lubow et al., 2014).

A within-subject design was employed and the *a priori* prediction was that conditioning to the pre-exposed stimulus (CS A−) would proceed more slowly than to a novel stimulus (Fig. 3A, C).

Both groups of *Gdi1* mice did not differ in the responses to the pre-exposed CS A− (ANOVA genotype effect: $F[1,14] = 0.016$; $p = 0.9$; Fig. 3B). Thus, we switched to the acquisition phase (Fig. 3C), where the CS A− became now rewarded (CS A+), randomly presented in between with a new CS (CS B+ non pre-exposed), in order to evaluate the strength of CS A− latent inhibition during pre-exposure stage. Both genotypes learnt and did not differ in the responses to the novel CS B+ (dotted lines) (ANOVA genotype effect: $F[1,14] = 0.17$; $p = 0.7$; Fig. 3D) providing further evidence of a similar hedonic response to appetitive conditioning. However, while in the *Gdi1* WT mice the former CS A− had an inhibitory effect on learning CS A+, this did not happen in *Gdi1*-null, which learnt the two CSs at the same rate (Fig. 3E). A significant interaction was observed between genotypes and day (ANOVA genotype × day: $F[3,1] = 3.3$; $p = 0.03$) and factorial analysis showed a significant difference between genotypes at day 9 (ANOVA factorial analysis day 9: $F[1,14] = 7.6$; $p = 0.015$), suggesting a lack of LI in the *Gdi1*-null group.

Gdi1-null mouse has an impaired ability to develop conditioned inhibition (CI)

We further investigated attention-related and inhibitory deficit since LI and CI share some basic features. While LI is seen as a loss of attention to the pre-exposed CS, during the CI an expected signaled food rewarded CS A is paired with a second CS C that is not rewarded and an active inhibition is formed.

In the first four days of acquisition (Fig. 4A, C left part of the graph), both genotypes responded equally to CS A+ (ANOVA genotype effect: $F[1,14] = 0.341$, $p = 0.57$) and to CS B+ (ANOVA genotype effect: $F[1,14] = 3.05$, $p = 0.1$) suggesting that both groups did not significantly differ in the acquisition phase and had similar hedonic response to food reward. Mice were then subjected to three days inhibitory training (fig. 4B, C right part of the graph) where a compound CS AC− was added to the previous two. Even in this inhibitory phase both groups quickly learnt to not respond to the CS AC− compound (ANOVA genotype effect for CS A: $F[1,14] = 0.096$; $p = 0.76$; CS B: $F[1,14] = 0.082$; $p = 0.78$; compound AC: $F[1,14] = 0.171$; $p = 0.69$). Next, on the following day (Fig. 4D, F) in a "Summation test" the *Gdi1*-WT group showed a trend to a greater suppression acquired in the previous stage for the conditioned inhibitor C (ANOVA genotype effect: $F[1,14] = 2$, $p = 0.1$). Yet on days 9 and 10 in the "Retardation test" (Fig. E, G), *Gdi1*-null mice were quicker in increasing their response to the former conditioned inhibitor CS C (ANOVA genotype effect: $F[1,14] = 9.1$; $p = 0.009$), indicating that the conditioned inhibition was not as effectively learnt as in the *Gdi1* WT.

This experiment demonstrates that while conditioning to stimuli had occurred equally in the first part of the test (Fig. 4A–C), CI ensued to a greater extent in *Gdi1* WT, as seen in the second part of the test (Fig. 4D-G), thus providing further evidence for a deficit in stimulus processing, and support for the LI results.

Dopamine release in the amygdaloidal nuclei is normal in *Gdi1*-null mouse

Most of the associative learning tasks are exclusively or at least largely dependent on the amygdaloidal nuclei as major brain structure involved in learning. Furthermore, reward learning and interval-timing behavior both involve dopamine release (Buhusi and Meck, 2006; Ward et al., 2009, 2012).

Hence to exclude a different hedonic state or a different valence of the US in *Gdi1*-null versus WT mice, we measured the ability of these mice to release dopamine in the amygdala (Galtress et al., 2012).

Synaptosomes prepared from *Gdi1*-null mice were comparable to those of *Gdi1*-WT mice for [^{3}H]DA total content (148290 ± 26759 vs 158991 ± 35644 d.p.m., $p = 0.8$). The spontaneous efflux of [^{3}H]DA was not different in the two animal groups (*Gdi1*-WT mice 2.19 ± 0.24%, $n = 8$; *Gdi1*-null mice 2.7 ± 0.26%, $n = 11$), as well as the 15 mM KCl-induced overflow of [^{3}H]DA (*Gdi1*-WT mice 2.23 ± 0.42%, $n = 8$; *Gdi1*-null mice 2.5 ± 0.46%, $n = 11$). These data clearly indicate that both genotypes have no difference in dopamine release in a key brain area underpinning associative reward learning.

Functional magnetic resonance imaging suggests modification of brain activity *in Gdi1*-null mice

To obtain a general overview of *Gdi1*-null brain function, we used a non-invasive *in vivo* imaging technique to support mechanistic hypotheses and yield information of translational relevance.

Structural MRI data obtained confirmed that gross cerebral morphology in *Gdi1* WT and *Gdi1*-null mice are alike and that the brain-wide lack of αGDI has no overt morphological consequences.

Functional MRI suggested that the brain perfusion, which was taken as a proxy for neural activity, tended to be different in some brain areas (Table 1, Fig. 5). Even though none of these differences reached statistical significance, altered neural activity of some potential relevance (i.e., $p < 0.20$) between *Gdi1*-null and *Gdi1* WT mice was observed in the dorsal peduncular (+14%), prelimbic (+8%) and infralimbic (+14%) cortices, the dorsal/ventral hippocampus (−6%), and the superior colliculus (−12%). However, no difference was seen in the striatum, which led us to further investigate its role in disease pathology at a more microscopic level.

Cortico-striatal synaptic vesicle readily releasable pool is reduced in *Gdi1*-null mice

Under the hypothesis that the neural substrate for the observed behavioral deficits is a reduced glutamatergic

Table 1. Brain areas examined by fMRI

Abbreviation	Brain area	Difference of neural activity *Gdi1*-null vs *Gdi1* WT (%)	*p*-Value
mPFC	Medial prefrontal cortex	4.23	0.45
PrL	Prelimbic cortex	8.27	0.13
IL	Infralimbic cortex	13.50	0.14
DP	Dorsal peduncular cortex	14.10	0.10
S1	Primary somatosensory cortex	0.56	0.93
S2	Secondary somatosensory cortex	0.56	0.90
M1	Primary motor cortex	−2.17	0.75
M2	Secondary motor cortex	1.90	0.75
V	Visual cortex	4.37	0.54
Ent	Entorhinal cortex	0.11	0.99
Ins	Insula cortex	−0.92	0.82
Str	Striatum	4.15	0.30
Acb	Accumbens nucleus	0.82	0.85
VP	Ventral pallidum	−1.36	0.85
BST	Bed nucleus of stria terminalis	0.54	0.90
VTA	Ventral tegmental area	−2.01	0.84
SNC	Substantia nigra	4.26	0.63
Ltha	Lateral thalamus	−4.59	0.57
Mtha	Median thalamus	−4.95	0.53
Amg	Amygdala	4.58	0.47
Hpc	Hippocampus	−1.89	0.43
Hpc (dv)	Hippocampus (dorsal + ventral)	−6.14	0.07
CA1	Hippocampus cornus ammonis 1	−0.51	0.88
S	Subiculum	1.23	0.68
DG	Hippocampus dentate gyrus	0.58	0.85
Sep	Septum	−0.23	0.95
dPAG	Dorsal periaqueductal gray	−3.20	0.70
vPAG	Ventral periaqueductal gray	−5.42	0.66
DR	Dorsal raphe nucleus	−2.89	0.78
MR	Medial raphe nucleus	8.92	0.54
SC	Superior colliculus	−12.10	0.12
LHyp	Lateral hypothalamus	−13.36	0.38
MHyp	Median hypothalamus	16.74	0.27

release in medial prefrontal-cortex (mPFC), whole-cell patch-clamp recordings were performed in *Gdi1* WT and *Gdi1*-null brain slices in order to investigate electrophysiological properties of excitatory cortico-striatal synapses and gather further evidence for the involvement of the fronto-striatal pathway.

The peak amplitude of individual EPSCs evoked in striatal MSNs by cortical extracellular stimulation was

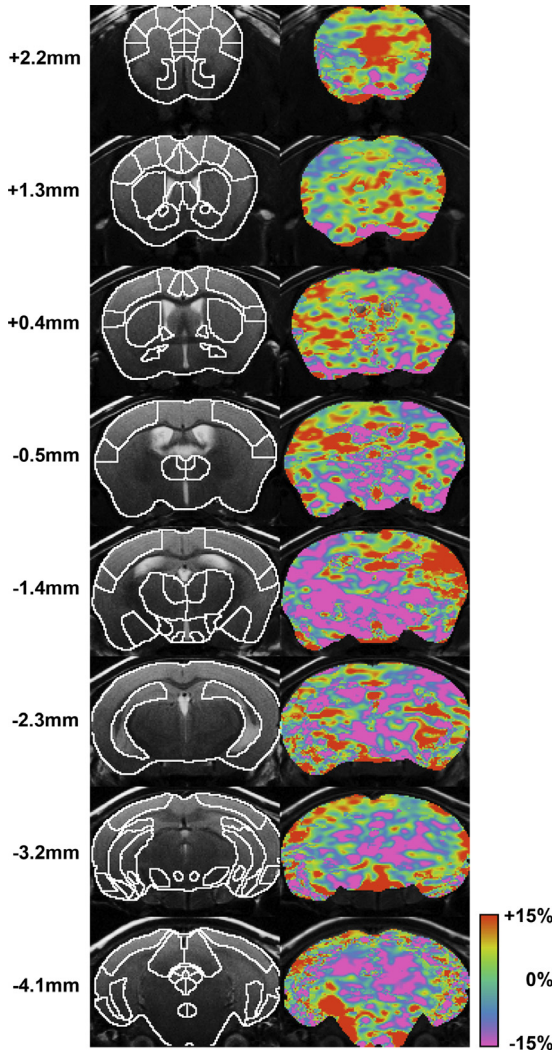

Fig. 5. Functional magnetic resonance imaging suggests brain region-specific alterations of neural activity in *Gdi1*-null mice. Left panel: anatomical images of the mouse brain acquired from eight coronal slices. The images are overlaid with a digital atlas defining 33 bilateral regions. The numbers indicate the distance to the bregma. Right panel: color-coded maps of normalized perfusion difference between *Gdi1*-null (n = 11) and *Gdi1*-WT mice (n = 7) at rest under etomidate anesthesia. Normalized perfusion was taken as a proxy for neural activity. Visually most prominent is an elevated activity in the infralimbic and prelimbic cortex of *Gdi1*-null mice. (For interpretation of the references to colour in this figure legend, the reader is referred to the web version of this article.)

significantly smaller in *Gdi1*-null than in *Gdi1* WT brain slices (206 ± 55 pA *vs.* 538 ± 108 pA, respectively, p = 0.011, n = 8, unpaired t test; Fig. 6A, B). Conversely, paired-pulse ratios did not change at any of the different inter-stimulus intervals tested (Fig. 6C), suggesting that the SV release probability was unaltered. Stimulation trains at high-frequency (20 Hz, 4 s) were then applied in order to construct EPSC amplitude cumulative plots and estimate the size of SV readily releasable pool (RRP; see Methods). The average RRP size was significantly smaller in *Gdi1*-null slices as compared to *Gdi1* WT slices (2.4 ± 0.4 nA *vs.* 8.0 ± 2.6 nA, respectively, p = 0.04, n = 6, unpaired t test; Fig. 6D, E), while the release probability (Pr) –

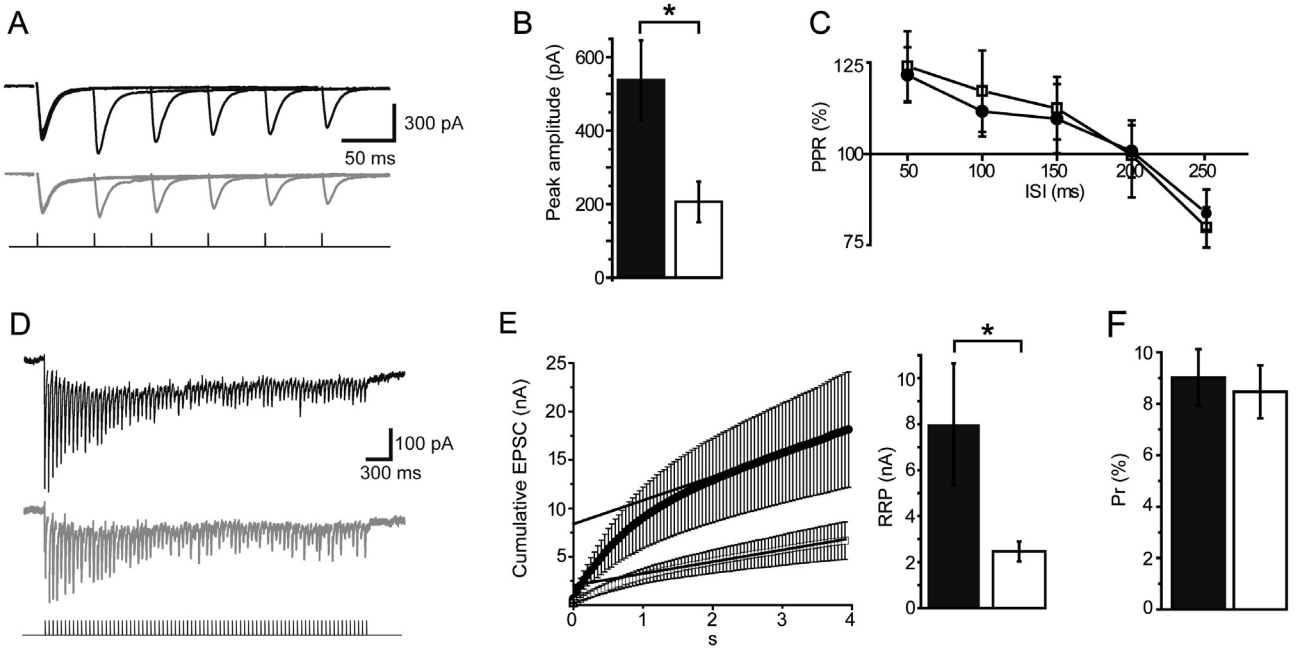

Fig. 6. The RRP size of synaptic vesicles is reduced in *Gdi1*-null cortico-striatal projections. (A) Representative traces showing superimposed EPSC responses to paired-pulse stimulations at various inter-stimulus intervals (ISIs; from 50 ms to 250 ms in 50-ms steps). Traces obtained from *Gdi1*-WT and *Gdi1*-null slices are shown in black and gray, respectively. (B) Summary histogram of average *Gdi1*-WT and *Gdi1*-null EPSC peak amplitudes. Data were obtained only from the first EPSC recorded in any paired-pulse stimulation protocol. (C) Mean paired-pulse ratios (PPR) plotted against ISIs. (D) Representative EPSC trains recorded in *Gdi1*-WT (black) and *Gdi1*-null (gray) MSNs in response to a high-frequency stimulus train (20 Hz, 4 s; shown in bottom trace). (E) Average cumulative plots of peak amplitudes of *Gdi1*-WT (black dots) and *Gdi1*-null (white squares) EPSCs. The straight lines represent linear extrapolations to the Y-axis intercept in order to obtain the RRP size (see Methods). (F) Average histograms of RRP sizes (*left*) and probability of vesicle release (Pr; *right*) calculated in 6 *Gdi1*-WT and 6 *Gdi1*-null MSNs. $^{*}p < 0.05$.

calculated by dividing the first EPSC in the train by the RRP size – was unaltered (*Gdi1*-WT: 9.0 ± 1.1%, *Gdi1*-null: 8.5 ± 1.0%, p = 0.7, *n* = 6, unpaired t test; Fig. 6F). Altogether, these data suggest that cortico-striatal synaptic transmission is weaker in *Gdi1*-null mice than in controls due to a smaller pool of readily releasable glutamatergic SVs.

DISCUSSION

In the present study, *Gdi1*-null mice were subjected to discriminative conditioning, interval-timing behavior, latent inhibition and conditioned inhibition in appetitive procedures to define the prominence of attention and fronto-striatal functional deficits similar to those reported in ID patients (Fernandez-Jaen, 2006; Aureli et al., 2010; Verhoeven et al., 2012).

Our results demonstrate that *Gdi1*-null mice, which show clear deficits in short-term and associative memory caused by alterations in the synaptic release machinery in glutamatergic terminals (Bianchi et al., 2009), are also impaired in appetitive Pavlovian conditioning paradigms.

Gdi1-null mice showed a poorer discriminative conditioning between a sound (CS) that predicted food (US) and one that did not in a delay-conditioning task. Since both groups showed a clear discrimination between the CS+ and CS-, the difference observed is likely not due to a poorer ability to discriminate different CSs, but rather caused by a change in the level of anticipatory response to the reward-predicting CS.

Gdi1-null mice were also poorer in timing task working memory that requires attention, stimulus processing ability and intact executive functions (Lustig et al., 2005; Meck et al., 2013; Merchant et al., 2013). The CS-onset first triggers a timing mechanism resulting in the information about the elapsed time being stored in working memory, and at the CS end this information on time duration has to be transferred to the long-term memory. Thus, the presentation of the same CS elicits the comparisons between the elapsing time with the remembered time and, when the comparison reaches the response threshold, the probability for triggering the action increases (Buhusi and Meck, 2005).

We then added a gap (a trace interval 5 s long) between a CS and US, in a discriminative conditioning preparation, and *Gdi1*-null mice showed a poorer conditioning to the CS interval (15 s long) while they did not for the trace. This is in general agreement with the overall hypothesis that *Gdi1*-null mice would perform worse than *Gdi1* WT in harder or longer tasks only. In fact our previous studies showed that a decreased SV reserve pool, which was demonstrated functionally by a slow recovery after SV depletion, leads to a memory deficit whenever the synaptic SV demand should increase both with task duration and difficulty (Bianchi et al., 2009). We also tested the Gdi1-null mice's ability in trace-peak procedure and also in this case the results

provided evidence of poorer interval timing and delayed peak position.

Conditioning deficit might likely be due to a poorer fronto-striatal and ventral tegmental area (VTA) interplay (Reichelt et al., 2013) and a reduced glutamatergic input from the mPFC as indicated by previous work (Schubert et al., 2015). With regard to interval timing, there is ample literature that indicates a critical role for the basal ganglia in temporal information processing and particularly of the striatum and its connections with the PFC and dopaminergic system (Buhusi and Meck, 2005; Valencia-Torres et al., 2012; Cope et al., 2014). Many studies indicate that temporal information processing can be distorted by manipulations that target the dopaminergic system (Buhusi and Meck, 2005). It has been suggested that striatal MSNs may serve as a monitor of neural activity in cortico-striatal circuits, and that they control working memory during interval timing tasks (Matell and Meck, 2004). Thus it has been hypothesized that a pulse of dopamine at the beginning of the interval to be timed triggers the MSNs, which monitor the oscillations in the firing of PFC neurons (Parker et al., 2011; Ward et al., 2012). When then a second pulse of dopamine signals the end of the interval the spatial pattern of firing in cortical neurons is stored by strengthening the currently engaged synapses (probably by a LTP mechanism), thus providing a memory of the interval duration (Meck et al., 2008).

Since PFC lesions produce distortions in timing (Olton, 1989; Picton et al., 2006) and modulate the effect of drugs that target striatal D2 receptors (Meck, 2006), it follows from the above reasoning that interval timing requires the integrity of cortico-striatal circuits which seem to be impaired by the lack of αGDI.

Finally, *Gdi1*-null mice showed attention-related learning deficits, demonstrated by using latent inhibition and conditioned inhibition paradigms. LI is a phenomenon that occurs when the pre-exposure to a stimulus reduces the speed with which it subsequently conditions and it is often regarded as a loss of attention to the pre-exposed cue (Mackintosh et al., 2010). On the other hand, CI is a phenomenon that occurs when a stimulus is learnt to signal the absence of an otherwise expected outcome. As a result, the inhibitor suppresses conditioned response to other signals for the reward and it is itself slower to become a signal than another CS.

In our LI protocol, where a pre-exposed CS was compared to a new CS, *Gdi1*-null mice showed a lack of LI since the pre-exposed stimulus was faster to acquire associative strength when compared to *Gdi1*-WT mice, which on the contrary showed LI.

In CI summation test, although the difference between groups was not sufficient to reach statistical significance, the ability of the light (C) to suppress response to B was greater in the *Gdi1*-WT mice. During the retardation test in which the conditioned inhibitor (C) itself was paired with food, here CI would be evident as slower learning, but *Gdi1*-null mice were faster to increase their response rate to C when compared to WT. Thus, *Gdi1*-null mice showed both LI and CI impairment that we believe to be due to a poorer functioning of the fronto-striatal pathway, because failure to show normal LI and CI has been considered a fronto-striatal function (Rhodes and Killcross, 2007; Green et al., 2011) and linked to the dopaminergic system as key substrate (Tobler et al., 2003; Bay-Richter et al., 2013). All together these data revealed marked behavioral deficits that are directly correlated to the fronto-striatal pathway and implicating glutamatergic system mal-functioning as the principal defect in neurotransmitter components.

Structural neuroimaging revealed that neuroanatomy, as expected, did not differ in *Gdi1*-null and *Gdi1* WT mice. Our fMRI assessments shed some light on potential functional differences and brain structures that tended to be hyper- or hypo-activated due to the lack of αGDI. It should be noted that these differences were observed at resting conditions where no phenotypical differences are otherwise apparent. It may be hypothesized that under conditions of increased cognitive workload, such as the behavioral paradigms reported here, the neuro-functional alterations become more overt. Notwithstanding, the current fMRI data are in alignment with the notion that prelimbic and infralimbic cortices might be more relevant in the temporal and reward processing underlying Pavlovian conditioning (Galtress et al., 2012).

To deeply investigate the role of fronto-striatal circuitry we then performed whole-cell recordings, which revealed significantly smaller individual glutamatergic EPSCs evoked by brief cortical stimulation and recorded in striatal MSNs. Such weaker transmission was not accounted for by a reduced probability of neurotransmitter release, but rather by a smaller sized pool of readily releasable synaptic vesicles as previously also described in the hippocampus.

As negative control for the validation of the experimental conditions in our model, we went then to investigate the release of dopamine in the amygdala because of the key role of dopamine in the above behavioral paradigms and the implication of the amygdala in associative and reward learning.

We demonstrated that dopamine release in the amygdala is normal in *Gdi1*-null mice, thus ruling out dopamine related differences in incentive value (Wassum et al., 2011; Kodama et al., 2014).

It shall also be noted that given the nature of the mutation in this mouse, it is highly unlikely that it has differentially affected dopamine release in other brain areas such as the striatum. However, we cannot exclude that other excitatory neurotransmitter systems or the inhibitory system might play a role in *Gdi1*-null mice cognitive phenotype and further analyses need to be carried out to evaluate also this aspect.

Taken together, these data provide strong supportive evidence for the hypothesis that the learning, memory and interval-timing deficits observed in *Gdi1*-null mice are mainly caused by a reduced glutamatergic release in cortical, striatal, amygdala and hippocampal brain areas. This finding suggests clinical studies in ID patients that investigate pharmacological treatments targeting and improving glutamatergic transmission.

FUNDING SOURCES

This study was supported by the Comitato Telethon Fondazione ONLUS (TCP04015) and by the Roche Postdoctoral Fellowship program (RPF #138, F. Hoffmann-La Roche AG, Switzerland).

FINANCIAL DISCLOSURES

None of the authors have financial disclosures or conflicts of interest pertinent to the contents of the manuscript, except for AB, SG and BK who received salaries as full-time employees with F. Hoffmann-La Roche AG.

Acknowledgments—We would like to thank Alessandro Nonis and Federica Cugnata in the group of Prof. Clelia di Serio at University Centre for Statistics in the Biomedical Sciences (CUSSB) at Università Vita Salute San Raffaele, Milan, Italy, for the valuable discussion on the issues arisen from the statistical analysis of this paper.

LM designed and carried out all the behavioral procedures with the help of VB. BK and AB performed fMRI. LY and ST performed electrophysiology. AM and EF performed dopamine release experiments. SG participated in the scientific discussion and paper revision. LM and PD wrote the manuscript.

REFERENCES

Aureli A, Del Beato T, Sebastiani P, Marimpietri A, Melillo CV, Sechi E, Di Loreto S (2010) Attention-deficit hyperactivity disorder and intellectual disability: a study of association with brain-derived neurotrophic factor gene polymorphisms. Int J Immunopathol Pharmacol 23:873–880.

Baker S, Hooper S, Skinner M, Hatton D, Schaaf J, Ornstein P, Bailey D (2011) Working memory subsystems and task complexity in young boys with Fragile X syndrome. J Intellect Disabil Res 55:19–29.

Balsam PD, Fairhurst S, Gallistel CR (2006) Pavlovian contingencies and temporal information. J Exp Psychol Anim Behav Process 32:284–294.

Bay-Richter C, O'Callaghan MJ, Mathur N, O'Tuathaigh CM, Heery DM, Fone KC, Waddington JL, Moran PM (2013) D-amphetamine and antipsychotic drug effects on latent inhibition in mice lacking dopamine D2 receptors. Neuropsychopharmacology 38:1512–1520.

Bexkens A, Ruzzano L, Collot D' Escury-Koenigs AM, Van der Molen MW, Huizenga HM (2014a) Inhibition deficits in individuals with intellectual disability: a meta-regression analysis. J Intellect Disabil Res 58:3–16.

Bexkens A, Van der Molen MW, Collot d'Escury-Koenigs AM, Huizenga HM (2014b) Interference control in adolescents with mild-to-borderline intellectual disabilities and/or behavior disorders. Child Neuropsychol 20:398–414.

Bianchi V, Farisello P, Baldelli P, Meskenaite V, Milanese M, Vecellio M, Muhlemann S, Lipp HP, Bonanno G, Benfenati F, Toniolo D, D'Adamo P (2009) Cognitive impairment in Gdi1-deficient mice is associated with altered synaptic vesicle pools and short-term synaptic plasticity, and can be corrected by appropriate learning training. Hum Mol Genet 18:105–117.

Bruns A, Kunnecke B, Risterucci C, Moreau JL, von Kienlin M (2009) Validation of cerebral blood perfusion imaging as a modality for quantitative pharmacological MRI in rats. Magn Reson Med 61:1451–1458.

Buhusi CV, Meck WH (2005) What makes us tick? Functional and neural mechanisms of interval timing. Nat Rev Neurosci 6:755–765.

Buhusi CV, Meck WH (2006) Time sharing in rats: a peak-interval procedure with gaps and distracters. Behav Processes 71:107–115.

Cope TE, Grube M, Singh B, Burn DJ, Griffiths TD (2014) The basal ganglia in perceptual timing: timing performance in Multiple System Atrophy and Huntington's disease. Neuropsychologia 52:73–81.

Curie A, Sacco S, Bussy G, de Saint Martin A, Boddaert N, Chanraud S, Meresse I, Chelly J, Zilbovicius M, des Portes V (2009) Impairment of cerebello-thalamo-frontal pathway in Rab-GDI mutated patients with pure mental deficiency. Eur J Med Genet 52:6–13.

Curie A, Brun A, Cheylus A, Reboul A, Nazir T, Bussy G, Delange K, Paulignan Y, Mercier S, David A, Marignier S, Merle L, de Freminville B, Prieur F, Till M, Mortemousque I, Toutain A, Bieth E, Touraine R, Sanlaville D, Chelly J, Kong J, Ott D, Kassai B, Hadjikhani N, Gollub RL, des Portes V (2016) A novel analog reasoning paradigm: new insights in intellectually disabled patients. PLoS One 11:e0149717.

D'Adamo P, Menegon A, Lo Nigro C, Grasso M, Gulisano M, Tamanini F, Bienvenu T, Gedeon AK, Oostra B, Wu SK, Tandon A, Valtorta F, Balch WE, Chelly J, Toniolo D (1998) Mutations in GDI1 are responsible for X-linked non-specific mental retardation. Nat Genet 19:134–139.

D'Adamo P, Welzl H, Papadimitriou S, Raffaele di Barletta M, Tiveron C, Tatangelo L, Pozzi L, Chapman PF, Knevett SG, Ramsay MF, Valtorta F, Leoni C, Menegon A, Wolfer DP, Lipp HP, Toniolo D (2002) Deletion of the mental retardation gene Gdi1 impairs associative memory and alters social behavior in mice. Hum Mol Genet 11:2567–2580.

Fernandez-Jaen A (2006) Attention deficit hyperactivity disorder and mental retardation. Rev Neurol 42(Suppl 2):S25–S27.

Gallistel CR, Balsam PD (2014) Time to rethink the neural mechanisms of learning and memory. Neurobiol Learn Mem 108:136–144.

Galtress T, Marshall AT, Kirkpatrick K (2012) Motivation and timing: clues for modeling the reward system. Behav Processes 90:142–153.

Green JT, Chess AC, Conquest CJ, Yegla BA (2011) Conditioned inhibition in a rodent model of attention-deficit/hyperactivity disorder. Behav Neurosci 125:979–987.

Grosshans BL, Ortiz D, Novick P (2006) Rabs and their effectors: achieving specificity in membrane traffic. Proc Natl Acad Sci U S A 103:11821–11827.

Kahn JB, Ward RD, Kahn LW, Rudy NM, Kandel ER, Balsam PD, Simpson EH (2012) Medial prefrontal lesions in mice impair sustained attention but spare maintenance of information in working memory. Learn Mem 19:513–517.

Kodama T, Hikosaka K, Honda Y, Kojima T, Watanabe M (2014) Higher dopamine release induced by less rather than more preferred reward during a working memory task in the primate prefrontal cortex. Behav Brain Res 266:104–107.

Lazar J, Kaplan O, Sternberg T, Lubow RE (2012) Positive and negative affect produce opposing task-irrelevant stimulus preexposure effects. Emotion 12:591–604.

Lubow RE, Kaplan O, Manor I (2014) Latent inhibition in ADHD adults on and off medication: a preliminary study. J Atten Disord 18:625–631.

Lubs HA, Stevenson RE, Schwartz CE (2012) Fragile X and X-linked intellectual disability: four decades of discovery. Am J Hum Genet 90:579–590.

Lustig C, Matell MS, Meck WH (2005) Not "just" a coincidence: frontal-striatal interactions in working memory and interval timing. Memory 13:441–448.

Mackintosh CG, Clark RG, Thompson B, Tolentino B, Griffin JF, de Lisle GW (2010) Age susceptibility of red deer (Cervus elaphus) to paratuberculosis. Vet Microbiol 143:255–261.

Matell MS, Meck WH (2004) Cortico-striatal circuits and interval timing: coincidence detection of oscillatory processes. Brain Res Cogn Brain Res 21:139–170.

Matell MS, Meck WH, Nicolelis MA (2003) Interval timing and the encoding of signal duration by ensembles of cortical and striatal neurons. Behav Neurosci 117:760–773.
Meck WH (2006) Frontal cortex lesions eliminate the clock speed effect of dopaminergic drugs on interval timing. Brain Res 1108:157–167.
Meck WH, Penney TB, Pouthas V (2008) Cortico-striatal representation of time in animals and humans. Curr Opin Neurobiol 18:145–152.
Meck WH, Church RM, Matell MS (2013) Hippocampus, time, and memory–a retrospective analysis. Behav Neurosci 127:642–654.
Merchant H, Harrington DL, Meck WH (2013) Neural basis of the perception and estimation of time. Annu Rev Neurosci 36:313–336.
Olton DS (1989) Frontal cortex, timing and memory. Neuropsychologia 27:121–130.
Parker JG, Beutler LR, Palmiter RD (2011) The contribution of NMDA receptor signaling in the corticobasal ganglia reward network to appetitive Pavlovian learning. J Neurosci 31:11362–11369.
Petrinovic MM, Hankov G, Schroeter A, Bruns A, Rudin M, von Kienlin M, Kunnecke B, Mueggler T (2016) A novel anesthesia regime enables neurofunctional studies and imaging genetics across mouse strains. Sci Rep 6:24523.
Petter EA, Lusk NA, Hesslow G, Meck WH (2016) Interactive roles of the cerebellum and striatum in sub-second and supra-second timing: Support for an initiation, continuation, adjustment, and termination (ICAT) model of temporal processing. Neurosci Biobehav Rev 71:739–755.
Pezze MA, Dalley JW, Robbins TW (2009) Remediation of attentional dysfunction in rats with lesions of the medial prefrontal cortex by intra-accumbens administration of the dopamine D(2/3) receptor antagonist sulpiride. Psychopharmacology 202: 307–313.
Picton TW, Stuss DT, Shallice T, Alexander MP, Gillingham S (2006) Keeping time: effects of focal frontal lesions. Neuropsychologia 44:1195–1209.
Raiteri M, Leardi R, Marchi M (1984) Heterogeneity of presynaptic muscarinic receptors regulating neurotransmitter release in the rat brain. J Pharmacol Exp Ther 228:209–214.
Reichelt AC, Exton-McGuinness MT, Lee JL (2013) Ventral tegmental dopamine dysregulation prevents appetitive memory destabilization. J Neurosci 33:14205–14210.
Rhodes SE, Killcross AS (2007) Lesions of rat infralimbic cortex result in disrupted retardation but normal summation test performance following training on a Pavlovian conditioned inhibition procedure. Eur J Neurosci 26:2654–2660.
Ropers HH, Hamel BC (2005) X-linked mental retardation. Nat Rev Genet 6:46–57.
Schalock RL, Verdugo MA, Gomez LE (2011) Evidence-based practices in the field of intellectual and developmental disabilities: an international consensus approach. Eval Program Plann 34:273–282.
Schneggenburger R, Meyer AC, Neher E (1999) Released fraction and total size of a pool of immediately available transmitter quanta at a calyx synapse. Neuron 23:399–409.
Schubert D, Martens GJ, Kolk SM (2015) Molecular underpinnings of prefrontal cortex development in rodents provide insights into the etiology of neurodevelopmental disorders. Mol Psychiatry 20:795–809.
Srivastava AK, Schwartz CE (2014) Intellectual disability and autism spectrum disorders: causal genes and molecular mechanisms. Neurosci Biobehav Rev 46(Pt 2):161–174.
Tobler PN, Dickinson A, Schultz W (2003) Coding of predicted reward omission by dopamine neurons in a conditioned inhibition paradigm. J Neurosci 23:10402–10410.
Valencia-Torres L, Olarte-Sanchez CM, Body S, Fone KC, Bradshaw CM, Szabadi E (2012) Fos expression in the orbital prefrontal cortex after exposure to the fixed-interval peak procedure. Behav Brain Res 229:372–377.
Verhoeven WM, Egger JI, Hoogeboom AJ (2012) X-linked Aarskog syndrome: report on a novel FGD1 gene mutation. Executive dysfunction as part of the behavioural phenotype. Genet Couns 23:157–167.
Ward RD, Kellendonk C, Simpson EH, Lipatova O, Drew MR, Fairhurst S, Kandel ER, Balsam PD (2009) Impaired timing precision produced by striatal D2 receptor overexpression is mediated by cognitive and motivational deficits. Behav Neurosci 123:720–730.
Ward RD, Kellendonk C, Kandel ER, Balsam PD (2012) Timing as a window on cognition in schizophrenia. Neuropharmacology 62:1175–1181.
Wassum KM, Ostlund SB, Balleine BW, Maidment NT (2011) Differential dependence of Pavlovian incentive motivation and instrumental incentive learning processes on dopamine signaling. Learn Mem 18:475–483.

(Received 4 October 2016, Accepted 23 December 2016)
(Available online 03 January 2017)